

Electron Paramagnetic Resonance and Optical Detection of Magnetic Resonance Studies of the Lowest Excited Triplet States of Purine, Benzimidazole, and Indazole in Benzoic Acid Host Crystals

Masayo NODA,[†] Shin-ichi NAGAOKA,^{††} and Noboru HIROTA*
 Department of Chemistry, Faculty of Science, Kyoto University, Kyoto 606
 (Received February 2, 1984)

The triplet states ($^3\pi\pi^*$) of purine, benzimidazole, and indazole are investigated in benzoic acid crystals by electron paramagnetic resonance (EPR) and optical detection of magnetic resonance (ODMR) techniques. Well resolved phosphorescence spectra were obtained at 4.2 K. The T_1 states of purine and benzimidazole are located at 26409 and 26536 cm^{-1} , respectively. The zero field splittings (ZFS) are $D=0.1042 \text{ cm}^{-1}$, $|E|=0.0608 \text{ cm}^{-1}$ for purine, and $D=0.1123 \text{ cm}^{-1}$, $|E|=0.0270 \text{ cm}^{-1}$ for benzimidazole. The decay rate constants of the triplet sublevels are determined at 1.5 K and are compared with those of indole. From the angular dependence of the EPR signals, the probable orientations of purine and benzimidazole in benzoic acid hosts are determined. From the observed hyperfine splittings (hfs) spin distribution of the T_1 state of purine is estimated. ($\rho_6=0.20$, $\rho_8=0.27$, and $\rho_2=0.12$). The effects of the nitrogen substitution in the pyrrole ring of indole on the ZFS and spin distribution are discussed.

The lowest excited triplet (T_1) states of purine, benzimidazole and indazole have received considerable attention because of their possible importance in photobiological processes. Numerous spectroscopic,^{1–9} EPR,^{10–12} ODMR, and theoretical^{13–15} investigations have been attempted before, but owing to poor solubility of these molecules in nonpolar solvents and difficulties in finding good host crystals, previous investigations have been limited severely. For example, neither well resolved phosphorescence spectra nor single crystal EPR spectra of the triplet states of these molecules have been reported.¹⁶ Zero field ODMR^{17–19} experiments have been made in rigid solution, but the sublevel schemes of the T_1 states as well as their decay properties are not completely understood. Details of the spin distributions in the T_1 states are also not known for these molecules.

In the course of investigations in this laboratory, we have found that benzoic acid (BAC) is a good host for polar molecules which are difficult to dissolve into the crystals of nonpolar molecules such as durene.²⁰ Therefore, we have attempted to investigate the properties of the T_1 states of purine, benzimidazole, indazole and indole in the mixed crystals of BAC by means of ODMR and EPR techniques in order to elucidate the properties of their T_1 states. Well-resolved phosphorescence spectra were obtained at 4.2 K, and the decay rate constants of the triplet sublevels as well as the zero field transition energies were determined at 1.5 K. Single crystal EPR experiments were also made to determine the sublevel schemes unambiguously and to obtain information about the spin distributions. Here we discuss the phosphorescence spectra, the zero field splittings (ZFS), the hyperfine splittings (hfs) and the sublevel decay properties of these molecules. Benzimidazole, indazole, and purine are also considered as nitrogen substituted indoles, respectively. In this work

it was found that the triplet properties are strongly affected by the nitrogen substitution of indole. We discuss the variations in the decay and magnetic properties in this series of molecules.

Experimental

Sample Preparation. BAC (Wako) was purified by extensive zone refining. Purine (Sigma) was purified by recrystallization from toluene followed by vacuum sublimation. Benzimidazole (Aldrich) and indole (Aldrich) were purified by vacuum sublimation. Indazole (Tokyo kasei) was recrystallized twice from water and then sublimated in vacuum. Mixed crystals of BAC with desired guest molecules were grown by the standard Bridgman method. About one percent of the guest molecule was contained in the initial melt, but the actual concentration of the guest is considered to be very low. The molecular structures of the guest molecules and the numbering systems used here are given in Fig. 1.

Phosphorescence and ODMR Experiments. Phosphorescence spectra were obtained with the ODMR setups described elsewhere.²¹ The ZFS and the decay rate constants were determined by the standard ODMR^{22,23} and microwave induced delayed phosphorescence (MIDP)²⁴ experiments made at 1.5 K. Since the sublevel lifetimes are relatively long in the present systems, the effect of the spin lattice relaxation probably cannot be neglected entirely even at 1.5 K. The experimental errors in the determination of k , are estimated to

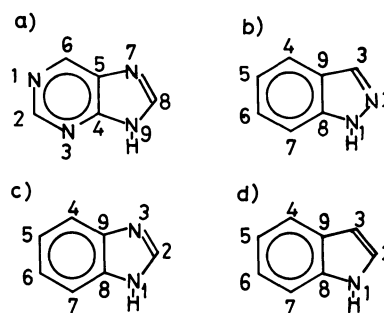


Fig. 1. Molecular structures and the numbering systems for a) purine, b) 1H-indazole, c) benzimidazole, d) indole.

Present address:

[†] Tokai Women's College, Kagamigahara, Gifu 504.

^{††} Division of Chemistry, Research Institute of Applied Electricity, Hokkaido University, Sapporo 060.

be $\sim 10\%$ and those of k_x and k_z are $\sim 25\%$. Microwave modulated phosphorescence spectra were obtained by applying the microwave at the ODMR transition frequencies and detecting the changes in the phosphorescence intensities, while the monochromator was scanned.

EPR Measurements. EPR measurements were made at 4.2 K with a JEOL JES-FE3X spectrometer with a home-built liquid helium cryostat. The experimental procedures are essentially the same as those described previously.²⁰ The crystal was mounted on a wedge so that the applied field rotated within the molecular plane of BAC by rotating the sample holder. The method of mounting a crystal was described elsewhere.¹⁶

Results and Discussion

Phosphorescence Spectra. The phosphorescence spectra of purine, benzimidazole and indazole in BAC obtained at 4.2 K are all well resolved as shown in Fig. 2. Since these molecules are expected to be in well defined configurations by forming hydrogen bonds with BAC, highly resolved spectra are probably obtained.

The O-O band of benzimidazole is very strong and is located at 376.9 nm. The frequencies of the main vibrations appearing in the phosphorescence spectra are in

good agreement with the ground state vibrational frequencies determined by IR and Raman studies as shown in Table 1. As discussed in detail in a separate paper,¹⁶ indazole in BAC exists in two tautomeric forms, 1*H*-indazole and 2*H*-indazole. The strong O-O band of the 1*H*-indazole spectrum is located at 423.9 nm. The observed vibrational frequencies are given in Table 1 together with the IR data.

The shortest wavelength band of the phosphorescence spectrum of purine in BAC appears at 368.85 nm, but the strongest band appears at 378.65 nm. The relative intensity of the former with respect to that of the latter depends on the sample preparation suggesting that the 368.85 nm band does not originate from purine. ODMR signals were observed at the bands with the wavelengths longer than 378.65 nm, but no ODMR signals were detected at the 368.85 nm band. The shorter wavelength portion of this spectrum resembles the corresponding portion of the phosphorescence spectrum of the BAC X-trap induced by anisole whose O-O band is located at 368.8 nm. (Fig. 2 c)-1) Therefore, it is concluded that the phosphorescence spectrum of purine in BAC is a superposition of the spectra coming from purine and the BAC X-trap. In order to eliminate the phosphorescence of the BAC X-trap and to obtain the genuine spectrum of purine, we have taken a microwave modulated phosphorescence spectrum. The spectrum obtained with the microwave modulation at 1.3 GHz is given in Fig. 2-d. It is seen that the spectrum has a very strong O-O band as those of benzimidazole and 1*H*-indazole. The main vibrational frequencies determined from the phosphorescence spectrum agree well with those determined from the IR and Raman spectra. (Table 1).

The strong O-O band observed here makes a striking contrast to the weak O-O bands found in the phosphorescence spectra taken in other environments, namely

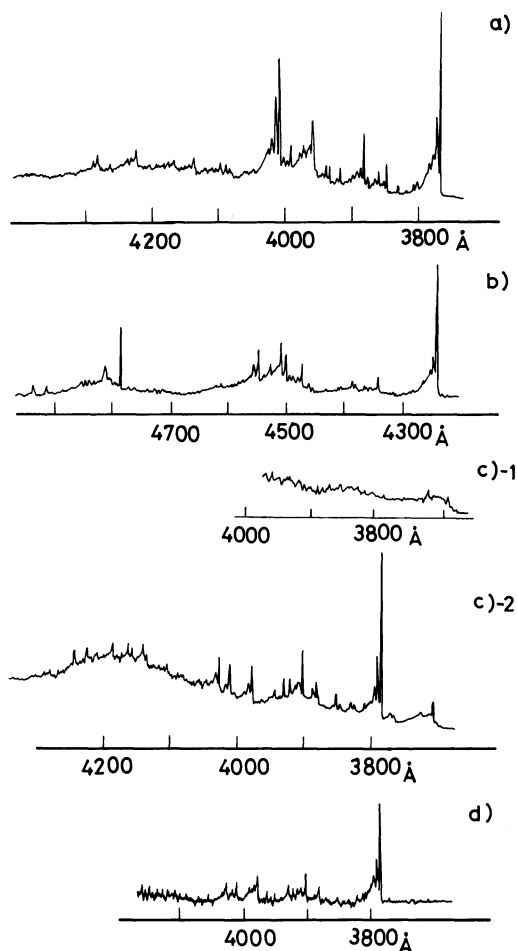


Fig. 2. Phosphorescence spectra in the mixed crystal of BAC at 4.2 K. a) benzimidazole, b) 1*H*-indazole, c)-1 benzoic acid X-trap, c)-2 purine, d) purine microwave modulated spectrum at 1.3 GHz.

TABLE 1. MAIN VIBRATIONAL BANDS APPEARING IN THE PHOSPHORESCENCE SPECTRA AND THE CORRESPONDING IR AND RAMAN BANDS

	Purine	Indazole	Benzimidazole
O-O	26409 cm ⁻¹	23590 cm ⁻¹	26536 cm ⁻¹
$\Delta\nu$ cm ⁻¹	446	549	548
	650 R 663		626 R 627
	780 R 795	775 IR 770	776 R 779
			IR 778
	909 IR 908		1010 R1006
			IR1004
	959 IR 963		1117 R1110
	1263 R1268	1224 IR1250	1274 R1274
			IR1274
	1480	1405 IR1380	1492 R1498
			IR1497
	1578 IR1565	1601 IR1605	1598 R1593
			IR1590

The Raman and IR frequencies for purine and indazole were determined in the present work. The values for benzimidazole were taken from Ref. 35.

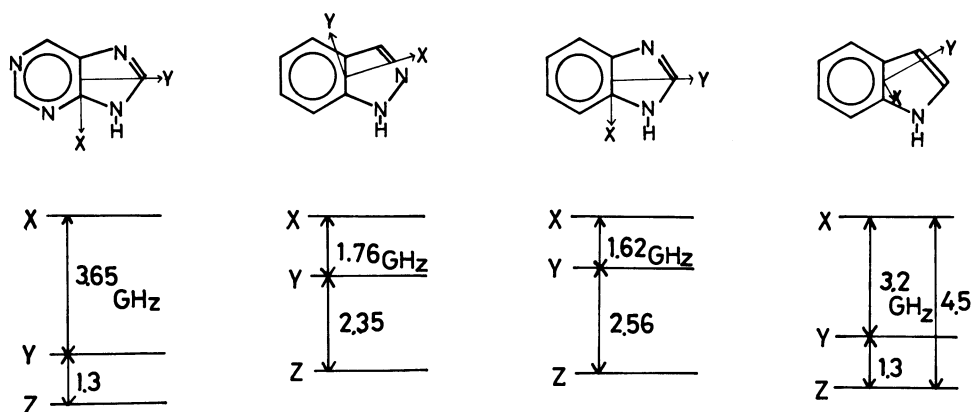


Fig. 3. Approximate direction of the principal axes of the ZFS and the sublevel schemes.

in a rare gas matrix,⁸⁾ powder,^{7,9)} and rigid solution.²⁾ The cause of this difference seems to be the following. While a well defined single site exists for purine in BAC, there are many sites with different O—O bands in other environments producing inhomogeneous broadenings of the spectra. In contrast to the sharp phosphorescence spectra of the above molecules, the spectrum of indole is very broad indicating the presence of prominent inhomogeneous broadening. The strong O—O bands and the relatively weak vibronic bands found for purine, benzimidazole, and indazole indicate that the structures of the T_1 states of these molecules are not much different from those of the ground states. The phosphorescence spectra of these three molecules are similar with the main vibronic bands at 0—780 cm^{-1} , 0—1270 cm^{-1} , and 0—1600 cm^{-1} (Table 1).

Sublevel Schemes and Zero Field Splittings. The ODMR signals were observed at 3.65 GHz and 1.30 GHz for purine, 2.56 GHz and 1.62 GHz for benzimidazole, 2.35 GHz and 1.76 GHz for 1H-indazole and 4.5 GHz, 3.2 GHz, and 1.3 GHz for indole, respectively. These ODMR frequencies correspond to the transitions between the sublevels which are eigenstates of the following spin Hamiltonian;

$$\begin{aligned}\mathcal{H} &= D\left(S_z^2 - \frac{1}{3}S^2\right) + E(S_x^2 - S_y^2) \\ &= -XS_z^2 - YS_y^2 - ZS_z^2,\end{aligned}\quad (1)$$

where $X=1/3D-E$, $Y=1/3D+E$ and $Z=-2/3D$.

Here we take the two in-plane spin axes as the X and Y axes. The Z axis is taken perpendicular to the molecular plane. The T_z sublevel is considered to be the bottom one as in the cases of other aromatic molecules. The top sublevel is taken as the X sublevel as shown in Fig. 3. We designate energies of the X, Y, and Z sublevels by T_x , T_y , and T_z , respectively.

The approximate directions of the X and Y axes were determined by the ratios of the radiative decay rate constants and the angular dependence of the EPR signals as discussed in the later sections. Whether $|T_y - T_z| > |T_x - T_y|$ or $|T_x - T_y| > |T_y - T_z|$ could not be determined from the ODMR experiments. In the former case $D > 3|E|$ and in the latter $D < 3|E|$. From the

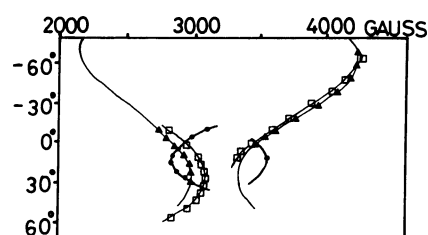


Fig. 4. Angular dependence of the EPR signals.

▲: Benzimidazole, □: 1H-indazole, ●: purine. The curves for benzimidazole and 1H-indazole are obtained by solving Eq. 2 with the ZFS determined by ODMR experiments. The curve for purine is drawn only for eye guide.

single crystal EPR experiments $D < 3|E|$ was established previously in the case of indole, and this was also tentatively assumed for the other molecules because of the similarities of the molecular structures.²⁵⁾ However, Svejda *et al.*¹⁸⁾ concluded $D > 3|E|$ for benzimidazole from the analysis of the decay data of the ODMR signals in ethanol. It is, therefore, desirable to determine the zero field sublevel schemes unambiguously and we have examined the angular dependence of the EPR signals of benzimidazole, 1H-indazole and purine in BAC. The mixed crystals were mounted so that the applied field rotated in the X-Y planes, on the assumption that the guest molecules substitutionally replace the host molecules. The obtained angular dependence curves are shown in Fig. 4. Unfortunately the signals were rather weak and we were only able to observe parts of the angular dependence curves, but they are sufficient to determine whether $D > 3|E|$ or $D < 3|E|$. It is immediately clear from Fig. 4 that $D > 3|E|$ in the case of benzimidazole and 1H-indazole, but $D < 3|E|$ in purine. The curves obtained for benzimidazole and 1H-indazole are in good agreement with those predicted by solving the spin Hamiltonian

$$\mathcal{H} = \beta H \cdot g \cdot S + DS_z^2 + E(S_x^2 - S_y^2) \quad (2)$$

with $g=2$ and the D and E values determined by the ODMR experiments. On the other hand, the agreement between the experimental and the predicted ones is poor for purine. This may be due to the deviation from the coplanarity of the guest and host molecules. The ZFS

determined in BAC are listed in Table 2 together with those determined in other hosts. The D and E values vary slightly depending on the host. $|E|$ of benzimidazole and 1*H*-indazole are smaller in BAC than in 1,4-dibromobenzene host (DBB), while $|E|$ of purine and indole are larger in BAC than in DBB. Though the ZFS are affected by the environment, the basic characters of the T_1 states are considered to remain unchanged on going from one environment to the other.

Decay Properties. The relatively long lifetimes of all the molecules studied here indicate that the T_1 states are $\pi\pi^*$ in character. We have determined the total decay rate constants (k_i) and the relative radiative decay rate constants (k_i^r) of the triplet sublevels by the MIDP experiments (Table 2). In spite of the poor molecular symmetries the decay constants are remarkably sublevel dependent; k_y and k_z^r are by far the largest in each molecule. The observation that k_z is similar to k_x seems to indicate the effect of spin lattice relaxation. The sublevel decay rate constants of purine, benzimidazole, and indole in ethanol were previously estimated by Moller and Nishimura¹⁷⁾ from the decomposition of the decay curves obtained at 1.5 K into three components. The sublevel decay constants of benzimidazole was determined in a mixture of ethylene glycol-water (1:1) by Svejda, *et al.*¹⁸⁾ and those of indole was also determined in the neat crystal by Zuclich *et al.*¹⁹⁾ The values obtained in the present work are somewhat different from those reported previously.

Benzimidazole, indazole, and purine are considered to be nitrogen substituted indoles. The decay rate constants of these molecules are larger than those of indole and this is presumably due to the presence of low lying $^1n\pi^*$ and $^3n\pi^*$ states which are brought in by the nitrogen substitution. These states mix with the T_1 ($^3\pi\pi^*$) states and enhance both radiative and nonradiative decay rates. The increase in the radiative decay rate due to the $^1n\pi^*$ state is determined by the spin-orbit matrix element $\langle ^1n\pi^* | \mathcal{H}_{so} | ^3\pi\pi^* \rangle$, the energy separation between the $^1n\pi^*$ and $^3\pi\pi^*$ state, $E(^1n\pi^*) - E(^3\pi\pi^*)$ and the transition moment $\vec{M}(^1n\pi^* - S_0)$. The increase in the nonradiative decay rate constant is determined by the energy separations $E(^3n\pi^*) - E(S_0)$, and $E(^3n\pi^*) - E(^3\pi\pi^*)$ and the spin-orbit matrix elements $\langle ^3n\pi^* | \mathcal{H}_{so} |$

$S_0 \rangle$ and $\langle ^1n\pi^* | \mathcal{H}_{so} | ^3\pi\pi^* \rangle$ as well as the matrix elements for vibronic couplings. In the present case spin-orbit matrix elements are mainly determined by the one center integral at the nitrogen atom.

When the one center integral at the nitrogen atom plays a dominant role in the relevant spin-orbit coupling matrix element for the increase in the radiative decay, the ratio of the increase in k_y^r (δk_y^r) to that in k_x^r (δk_x^r) is given by²⁶⁾

$$\delta k_y^r / \delta k_x^r = \cos^2 \alpha / \sin^2 \alpha \quad (3)$$

where α is the angle between the X axis and the direction of the nitrogen lone pair orbital. A similar equation holds for the nonradiative decay. The data given in Table 2 show that the increases in the decay rates on going from indole to benzimidazole and 1*H*-indazole are mainly in k_y . Then the direction perpendicular to the lone pair orbital of the nitrogen atom must be close to the direction of the Y axes. This means that the Y axis of benzimidazole is along the direction of the long molecular axis as shown in Fig. 5, whereas that of 1*H*-indazole is along the short axis.

Because of the nitrogen substitution in the six-membered ring k_y of purine is larger than those of

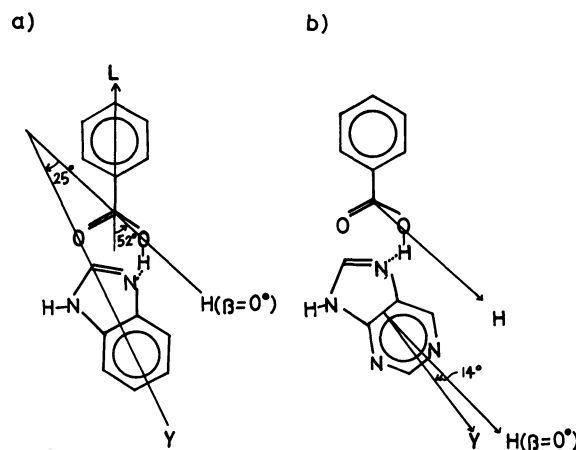


Fig. 5. The probable orientations of a) benzimidazole and b) purine in BAC. The dotted lines indicate hydrogen bonds.

TABLE 2. ZERO FIELD SPLITTING PARAMETERS AND THE DECAY RATE CONSTANTS OF SUBLEVELS

		Purine	Indazole	Benzimidazole	Indole
D cm ⁻¹		0.1042 (0.1009) ^{a)} (0.0990) ^{b)}	0.1077 (0.1073) ^{a)}	0.1123 (0.1178) ^{a)} (0.1185) ^{b)}	0.0967 (0.0978) ^{a)}
$ E $ cm ⁻¹		0.0608 (0.0584) ^{a)} (0.0647) ^{b)}	0.0293 (0.0310) ^{a)}	0.0270 (0.0362) ^{a)} (0.0325) ^{b)}	0.0533 (0.0453) ^{a)}
k_i sec ⁻¹	x	0.29	0.13	0.08	0.1
	y	2.1	0.85	0.57	0.3
	z	0.22	0.16	0.095	0.09
k_i^r	x	0.2	0.05	<0.1	<0.1
	y	1	1	1	1
	z	0.2	0.09	0.11	0.1

a) DBB, Ref. 25. ZFS are recalculated based on the sublevel scheme determined in this work. b) Ethylene glycol-water (1:1), Ref. 18.

TABLE 3. ENERGIES OF THE $^3\pi\pi^*$, $^1n\pi^*$, AND $^1\pi\pi^*$ STATES AND THE LARGEST SUBLEVEL DECAY RATE CONSTANTS

	$E(^3\pi\pi^*)$ cm ⁻¹	$E(^1n\pi^*)$ cm ⁻¹	$E(^1\pi\pi^*)$ cm ⁻¹	$E(^1n\pi^*) - E(^3\pi\pi^*)$ cm ⁻¹	k_y sec ⁻¹
Purine	26409	31408 ^{e)}		4499	2.1
Benzimidazole	26539	>35732 ^{e)}	36023 ^{b)}	>9193	0.57
Indazole	23590	>33272 ^{e)}	34473 ^{d)}	>9682	0.85
Indole	24135 ^{a)}		35233 ^{d)}		0.30
Quinoxaline	21639 ^{b)}	27070 ^{f)}	31950	5431	11.1 ^{b)}
Quinoline	21700 ^{c)}	29656 ^{g)}		7956	3.1 ^{c)}
Isoquinoline	21268 ^{d)}	30921 ^{g)}		9653	3.0 ^{d)}
Naphthalene					0.65 ^{k)}

a) Ref. 25. b) Ref. 36. c) and d) S. Yamauchi private communications. e) Ref. 7. f) Ref. 37. g) Ref. 38.
h) Ref. 39. i) Ref. 40. j) Ref. 41. k) Ref. 42.

benzimidazole and indazole. The one center integrals at the nitrogen atoms 3 and 7 are considered to be important in determining the spin-orbit matrix elements because of a smaller spin density expected at the nitrogen atom 1. The Y axis of purine is also expected to be along the long axis of the molecule.

The increase of k_y on going from indole to benzimidazole, indazole, and purine are 0.27 sec⁻¹, 0.55 sec⁻¹, and 1.8 sec⁻¹, respectively. The difference between benzimidazole and indazole may be primarily due to the increased nonradiative decay rate constant of indazole because $E(T_1) - E(S_0)$ of indazole is smaller than that of benzimidazole by ~ 3000 cm⁻¹. The increase in the case of purine can be attributed to the increased spin-orbit matrix element due to the inclusion of two nitrogen atoms in the six-membered ring and smaller energy separations between the $^3\pi\pi^*$ state and the $^1n\pi^*$ and $^3n\pi^*$ states.

The observed increases in the decay rate constants by the nitrogen substitution in the indole skeleton are, however, rather small when we compare them with the increases found for the nitrogen substitution in naphthalene. In Table 3 we compare the increases found for the present systems with those found for a series of molecules, quinoline, isoquinoline, and quinoxaline. As seen from the Table 2 the increases are about five times smaller for the present series.

The deuteration of purine reduces the decay rate constants, with $k_y[D]/k_y[H]=0.62$. This ratio is similar to that found for quinoxaline, $k_y[D]/k_y[H]=0.6$.^{24c)} The reduction of the decay rate constant is due to the decrease of the nonradiative decay rate constant. In the case of quinoxaline the ratio of the radiative and the nonradiative decay rate constants, $k_r:k_{nr}$ is estimated to be 5:7.²⁷⁾ As in the case of quinoxaline the nonradiative decay is considered to occupy a significant part of the total decay in the case of purine. Then it is concluded that the increases in both radiative and nonradiative decay rate constants are much larger in the naphthalene series. Since energy denominators $E(^1n\pi^*) - E(^3\pi\pi^*)$ are similar for the both series, the differences in the spin-orbit matrix elements $\langle ^1n\pi^* | \mathcal{H}_{so} | ^3\pi\pi^* \rangle$ and the transition moment \mathbf{M} are likely to be responsible for the differences in the radiative decay rate constants. As to the nonradiative

decay the increased Franck-Condon factor due to the smaller $E(T_1) - E(S_0)$ probably enhances the nonradiative decay in the naphthalene series.

Orientations of Guest Molecules and Hyperfine Interactions.

We measured the angular dependence of the EPR signals from the point at which the cleavage plane is in the direction of the applied field. At this orientation the direction of the applied field is rotated by 52° from the direction of the long axis (L axis) of BAC as shown in Fig. 5. We measure the rotation angle (β) of the applied field from this point. The Y stationary point of benzimidazole is obtained at $\beta=25^\circ$. In the same way the Y stationary point of purine is found at $\beta=14^\circ$. As discussed in the last section the Y directions of benzimidazole and purine are along the long axes of the molecules. Then the approximate orientations of these molecules in the BAC host are given as shown in Fig. 5. These orientations are consistent with the hydrogen bonded structures.

Hfs of purine is obtained at its Y stationary point. (Fig. 6) This hfs comes from the protons because the in-plane nitrogen hyperfine coupling constants (hfcc) are expected to be small.²⁸⁾ Using a Gaussian line shape for each hyperfine component, we simulate this spectrum with three coupling constants; 7.5, 4.2, and 3.2 G as shown in Fig. 6. We consider the hfs of the protons attached to the carbons 2, 6, and 8, since the spin density at N₉ is expected to be very small. When the applied field makes an angle θ with the direction perpendicular to the C-H direction, the hfcc of a proton in the $m_s=0 \leftrightarrow m_s=1$ transition is given by

$$\Delta h(\beta) = [(\rho A_{xz} \cos^2 \theta - \rho A_{yz} \sin^2 \theta - g_n \beta_n H)^2 + \frac{\rho^2}{4} (A_{xz}^2 - A_{yz}^2) \sin^2 2\theta]^{1/2} - g_n \beta_n H. \quad (4)$$

Here $A_{xx}=-36.5$ G, $A_{yy}=-11.5$ G, and $A_{zz}=-23.5$ G^{29,30)} are the principal values of the hyperfine tensor of a proton attached to an aromatic carbon. (x and y are perpendicular and parallel to the C-H direction in the molecular plane, respectively. \hat{z} is perpendicular to the molecular plane.) Since C₆-H is nearly perpendicular to the direction of the applied field at the Y stationary point, the largest hfcc 7.5 G is likely due to the proton at position 6. $\rho_6=0.20$ is immediately

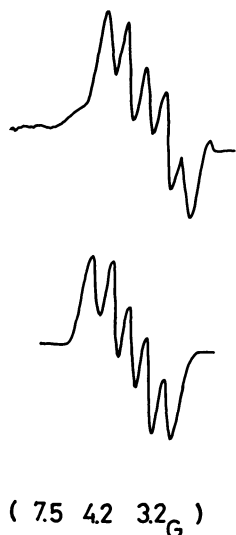


Fig. 6. Hyperfine structure in the EPR spectrum of purine in BAC. H/Y ($\beta=0^\circ$). Upper: experimental, lower: simulated.

obtained from Eq. 4 with $\theta=0^\circ$. C₈-H is nearly parallel to the applied field and the hfcc is expected to be small. So we may consider the smallest hfcc 3.2 G is due to the proton at position 8. $\rho_8=0.27$ is obtained from Eq. 4 with $\theta=90^\circ$. The remaining hfcc 4.2 G is then assigned to the proton at position 2. ρ_2 is given to be 0.12 from Eq. 4 with $\theta=60^\circ$.

Magnetic Properties and the Nature of the Triplet States. One remarkable observation is that $|E|$ of benzimidazole and 1H-indazole are much smaller than that of $|E|$ of indole, despite the similarity of their structures. This indicates that the nitrogen substitution to the pyrrole ring of indole modifies the nature of the T₁ state drastically. In the previous work²⁵ it was shown that the ZFS and the nature of the T₁ state of indole are very similar to those of indene and benzofuran which are viewed as substituted benzenes with strongly mesomeric substituents. The large $|E|$ was attributed to a large delocalization of the unpaired electron into the -C=C- groups of the five-membered ring. On the other hand, much smaller $|E|$ values found for benzimidazole and 1H-indazole indicate that the delocalization of the unpaired electron into the -C=N- groups is much less. The T₁ states of these molecules are approximately described by the excitation of an electron from the highest occupied molecular orbital (HOMO) to the lowest unoccupied molecular orbital (LUMO). The HOMO and LUMO of benzimidazole and 1H-indazole then must be very different from those of indole. The observed difference in the spin distributions also indicates this. It was suggested that in indole $\rho_4 \approx \rho_8 \approx 0.5\rho_6$, $\rho_3 < \rho_6$, and that ρ_5 and ρ_7 are small.²⁵ The analysis of the hfs in 1H-indazole indicates that ρ_4 , ρ_7 , and ρ_5 are large,¹⁰ showing that the HOMO and LUMO of indole are strongly affected by the nitrogen substitution.

The ZFS and the spin distribution of purine are expected to be different from those of other in this series

because of the presence of two nitrogen atoms in the six-membered ring. Here D is similar to those of others, but $|E|$ is very large, indicating larger spin densities in the -C=H- groups of the five-membered ring. The spin distribution in the triplet state is also very different from that of the purine anion. In the purine anion ρ_6 is very large ($\rho_6=0.44$),³¹ but in the triplet state ρ_6 (0.20) is smaller than ρ_8 (0.27). ρ_8 in the anion is smaller than that in the triplet state. A simple π electron MO calculation indicates that the HOMO and the LUMO of purine are very different and that the spin distributions of the anion and the triplet state are very different. This expectation is born out experimentally. This difference in the spin distributions makes a marked contrast to the cases of many aromatic molecules in which the spin distributions in the triplet states are similar to those of anions.^{30,32-34}

References

- 1) H. U. Schutt and H. Zimmerman, *Ber. Bunsenges. Phys. Chem.*, **67**, 54 (1963).
- 2) B. J. Cohen and L. Goodman, *J. Am. Chem. Soc.*, **87**, 5487 (1965).
- 3) C. Cailly and A. Boukhors, *C. R. Hebd. Seances Acad. Sci., Ser. C*, **264**, 480 (1967).
- 4) P. Loustauneau, *J. Chim. Phys. Phys-Chim. Biol.*, **68**, 1675 (1971).
- 5) B. S. Kirkiacharian, R. Santus, and C. Helen, *Photochem. Photobiol.*, **16**, 455 (1972).
- 6) J. W. Longworth, R. O. Rahn, and R. G. Shulman, *J. Chem. Phys.*, **45**, 2930 (1966).
- 7) M. J. Robey and I. G. Ross, *Photochem. Photobiol.*, **21**, 363 (1975).
- 8) J. J. Smith, *Spectrochimica Acta, Part A*, **33**, 135 (1977).
- 9) Drobnik, J. and L. Augenstein, *Photochem. Photobiol.*, **5**, 13 (1966).
- 10) B. Smaller, *J. Chem. Phys.*, **37**, 1578 (1962).
- 11) C. Helen, R. Santus, and P. Douzou, *Photochem. Photobiol.*, **5**, 127 (1966).
- 12) J. Zuclich, *J. Chem. Phys.*, **52**, 3586 (1970).
- 13) A. Pullman and E. Kochanski, *Int. J. Quantum Chem.*, **15**, 251 (1967).
- 14) E. Kochanski and A. Pullman, *Int. J. Quantum Chem.*, **3**, 1055 (1969).
- 15) J. Zuclich, *J. Chem. Phys.*, **52**, 3592 (1971).
- 16) Parts of the results on 1H-indazole was reported in a recent related paper. M. Noda and N. Hirota, *J. Am. Chem. Soc.*, **105**, 6790 (1983).
- 17) G. Moller and A. M. Nishimura, *J. Phys. Chem.*, **81**, 147 (1977).
- 18) P. Svejda, R. R. Anderson, and A. H. Maki, *J. Am. Chem. Soc.*, **100**, 7131 (1978).
- 19) J. Zuclich, J. U. Schutz, and A. H. Maki, *Mol. Phys.*, **28**, 33 (1974).
- 20) S. Nagaoka and N. Hirota, *J. Chem. Phys.*, **74**, 1637 (1981).
- 21) T. H. Cheng and N. Hirota, *J. Chem. Phys.*, **56**, 5019 (1972).
- 22) D. S. Tinti, M. A. El-Sayed, A. H. Maki, and C. B. Harris, *Chem. Phys. Lett.*, **3**, 343 (1969).
- 23) J. Schmidt and J. H. van der Waals, *Chem. Phys. Lett.*, **3**, 546 (1969).
- 24) a) J. Schmidt, W. S. Veeman, and J. H. van der Waals, *Chem. Phys. Lett.*, **4**, 341 (1969).
- b) D. A. Anthéunis, J. Schmidt, and J. H. van der Waals, *Chem. Phys. Lett.*, **6**, 355 (1970); c) *Mol. Phys.*, **22**, 1 (1971).

- 25) E. T. Harrigan and N. Hirota., *J. Am. Chem. Soc.*, **97**, 6647 (1975).
 - 26) D. A. Antheunis, B. J. Botter, J. Schmidt, and J. H. van der Waals, *Mol. Phys.*, **29**, 49 (1975).
 - 27) R. Li and E. C. Lim, *J. Chem. Phys.*, **57**, 605 (1972).
 - 28) J. S. Vincent, *J. Chem. Phys.*, **52**, 3714 (1970).
 - 29) Ph. J. Vergragt, J. A. Kooter, and J. H. van der Waals, *Mol. Phys.*, **33**, 1523 (1977).
 - 30) N. Hirota, C. A. Hutchison, and P. Palmer, *J. Chem. Phys.*, **40**, 3717 (1964).
 - 31) H. Ohya-Nichiguchi, Y. Shimizu, N. Hirota, and K. Watanabe, *Bull. Chem. Soc. Jpn.*, **53**, 1252 (1980).
 - 32) N. Hirota, T. C. Wong, and E. T. Harrigan, *Mol. Phys.*, **29**, 903 (1975).
 - 33) R. H. Clarke and C. A. Hutchison, *J. Chem. Phys.*, **54**, 2962 (1971).
 - 34) R. P. Forsch, A. M. Ponte-Goncalves, and C. A. Hutchison, *J. Chem. Phys.*, **58**, 5209 (1973).
 - 35) B. Borah and J. L. Wood, *Can. J. Chem.*, **54**, 2470 (1976).
 - 36) McCleu, *J. Chem. Phys.*, **17**, 965 (1949).
 - 37) R. W. Glass, L. C. Robertson, and J. A. Merrit, *J. Chem. Phys.*, **53**, 3857 (1970).
 - 38) H. Moriyama, Y. Udagawa, and M. Iroh, Abstract of the Symposium on Molecular and Electronic Structures, Hokkaido, 1977 P 452.
 - 39) R. D. Gordon and R. F. Yang, *Can. J. Chem.*, **48**, 1722 (1979).
 - 40) J. P. Byrne and I. G. Ross, *Aust. J. Chem.*, **24**, 1107 (1971).
 - 41) J. M. Hollas, *Spectrochim. Acta*, **19**, 753 (1963).
 - 42) M. Schwoerer and H. Sixl, *Chem. Phys. Lett.*, **2**, 14 (1968).
-